Thermally-Driven Interface Engineering of PMo_{12}/BiOBr Heterojunctions for Enhanced Artificial Photosynthesis of CO_2 in water vapor

Yan Shi,[a] Shiqin Liu,[a] Hui Chen,[a] Zaihui Fu, [b] Youji Li,[a] Senpei Tang*[a]

[a] *Hunan Province Key Laboratory of Mineral Cleaner Production And Green Functional Materials, College of Chemistry and Chemical Engineering, Jishou University, Jishou, 416000, Hunan, PR China*

[b] *College of Chemistry and Chemical Engineering, Hunan Normal University, 410081, Hunan, PR China*

Experimental section

Reagent

All materials and reagents employed in this investigation analytical grade, comprising bismuth nitrate pentahydrate ($Bi(NO_3)_3 \cdot 5H_2O$, 99%), potassium bromide (KBr, 99%), phosphomic heteropoly acid ($H_3PMo_{12}O_{40}$), ethanol (CH_3CH_2OH, 99.0%), and tetrabutylammonium hexafluorophosphate ($TBAPF_6$, 98%). Deionized water served as the aqueous medium throughout all experimental procedures.

Characterization

Crystal structure characterization was performed using a Bruker D8 Advance X-ray diffractometer (XRD) with Cu-K_α radiation (λ=1.5406 Å) in the 2θ range of 10°–80°. UV-vis diffuse reflectance spectra (DRS) were recorded on a Shimadzu UV-1900i spectrophotometer (200-800 nm wavelength range). Morphological analysis was conducted using a Zeiss Gemini 300 field-emission scanning electron microscope (SEM). Elemental composition and chemical states were determined by Thermo Scientific K-Alpha X-ray photoelectron spectroscopy (XPS). Fourier transform infrared (FT-IR) spectra were acquired using a Vertex 70 spectrometer (4000-400 cm^{-1}).

* Corresponding author E-mail address: ChemTangJSU@163.com (Senpei Tang)

Catalyst synthesis

Synthesis of BiOBr: $Bi(NO_3)_3 \cdot 5H_2O$ (4 mmol) was dissolved in 50 mL deionized water with stirring for 0.5 h. A KBr solution (4 mmol in 20 mL H_2O) was then added dropwise to the solution with continued stirring for 0.5 h. The mixture was transferred to a 100 mL Teflon-lined autoclave and hydrothermally treated at 160 °C for 12 h. After cooling to room temperature, the product was washed with deionized water and ethanol three times, then dried at 60 °C for 24 h to obtain BiOBr (denoted as BOB).

Synthesis of t_n-PM/BOB_x composites: As shown in Fig. S1, $H_3PM_{12}O_{40}$ (PM, 0.1 g) and BOB (0.1 g) were homogeneously ground in an agate mortar for 15 min at 120 rpm rotational frequency. The homogenized mixture was transferred to a alumina combustion boat and calcined in a tube furnace with continuous gas flow (200 mL/min) using a precisely controlled thermal protocol: ramping from room temperature to 200 °C at 5 °C/min, followed by 2 h isothermal annealing. Post-calcination, the system was cooled to 30 °C at 10 °C/min, yielding a green solid denoted as t_n-PM/BOB_x, where the subscript "n" represents calcination temperatures (25, 100, 150, 200, 220, 250, 300 °C), and "x" indicates the mass ratio of BOB in the composite (0.16, 0.25, 0.5, 0.75, 0.8).

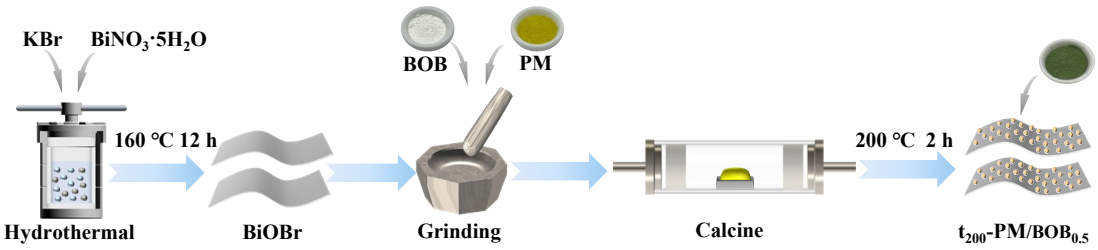

Fig. S1 Schematic diagram of synthesis process of t_n-PM/BOB_x.

Evaluation of photocatalytic CO_2 reduction performance

A catalyst (10 mg) was dispersed in 1 mL deionized water via sonication. The suspension was deposited onto a circular glass substrate (2 cm diameter) using a spin-coating method, followed by ambient drying for 12 h to form a uniform catalytic film. This film was then suspended in a gas-tight quartz reactor containing 5 mL deionized water, ensuring physical separation between the film and aqueous phase (Fig. S2a). Prior to illumination, the reactor was evacuated to remove residual air and purged with

high-purity CO_2 (99.999 %). The total volume of the reactor with gas pipelines is 550 mL. The CO_2 partial pressure in the reactor was maintained within the range of 2.0-18.4 kPa (2-18 vol%), with a stable flow velocity of 20 mL·min^{-1}. Temperature control was maintained at 25±5 °C using a recirculating chiller system. Photocatalytic reactions were driven by a 300 W xenon lamp equipped with an AM 1.5G filter (light intensity: 117.22 mW·cm^{-2}). Reaction products were automatically sampled at 30-min intervals through an online gas chromatograph (GC9790plus, FULI INSTRUCMENTS, China) equipped with a FID. Quantification was performed using pre-calibrated standard curves as detailed in Fig. S2b.

Characterization of photochemical properties

The catalyst (10 mg) was ultrasonically dispersed in 2 mL ethanol containing 30 μL Nafion solution (5 wt%) to form a homogeneous suspension, followed by immersion of a 1×2 cm FTO glass substrate into the mixture. Uniform catalyst loading was achieved via centrifugation at 8000 rpm, and the coated substrate was air-dried to form a catalytic film. Photoelectrochemical measurements were conducted in a three-electrode system (Pt counter electrode, Ag/AgCl reference electrode) using 0.25 mmol·L^{-1} tetrabutylammonium hexafluorophosphate as electrolyte under illumination from a 300 W xenon lamp. Transient photocurrent (PTC) was recorded over 200 s with 20 s light chopping intervals, while electrochemical impedance spectroscopy (EIS) and Mott-Schottky (M-S) analyses were performed in frequency ranges of 0.01 Hz–100 kHz and potential windows of OCP ±1 V, respectively, utilizing a CHI 660I electrochemical workstation.

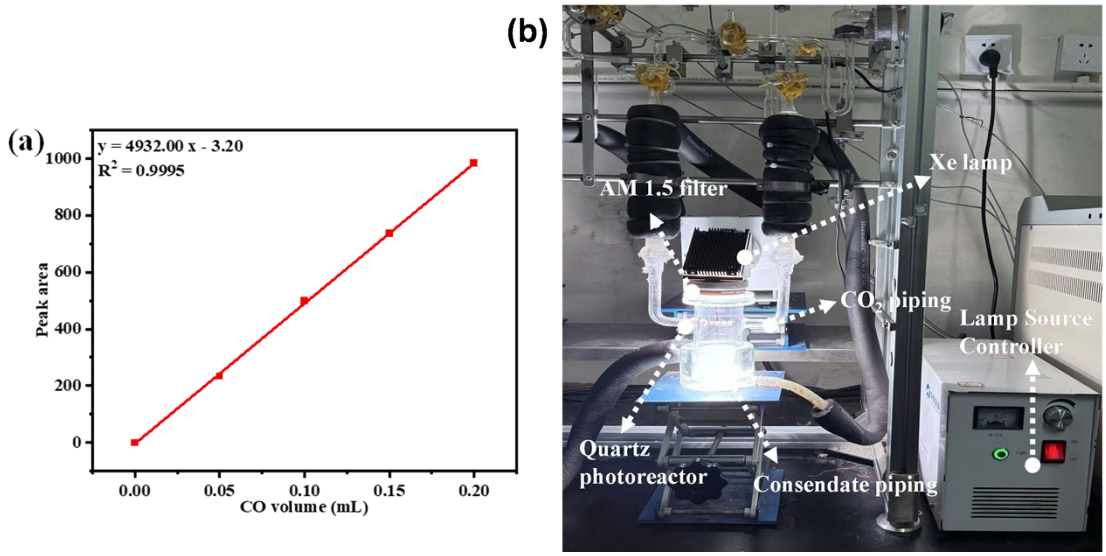

Fig. S2. (a) CO quantification standard curve derived from gas chromatography analysis and (b) Photos of the photocatalytic CO_2 reduction reactor

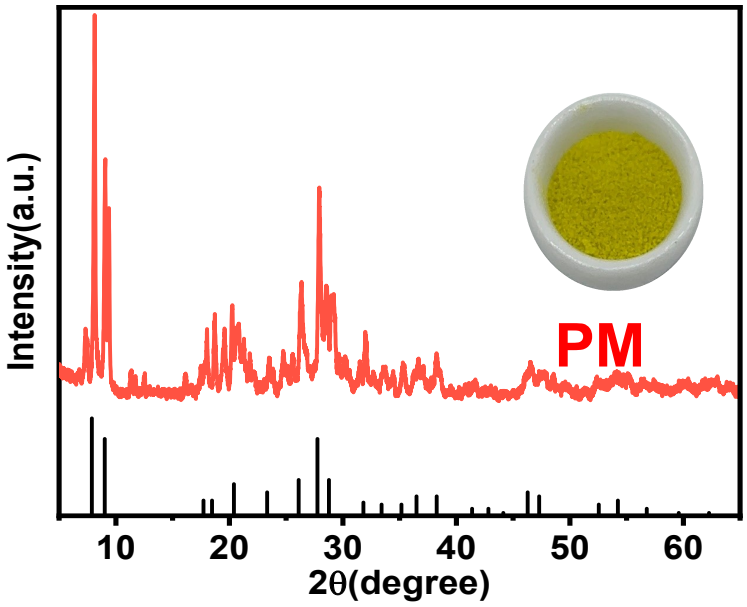

Fig. S3 The XRD pattern of PM, and inset is photograph of yellow PM powder.

Fig. S4 Color change diagram of catalyst t_n-PM/$BOB_{0.5}$ (n= 25, 100, 150, 200, 220, 250, 300 ℃) at different temperatures

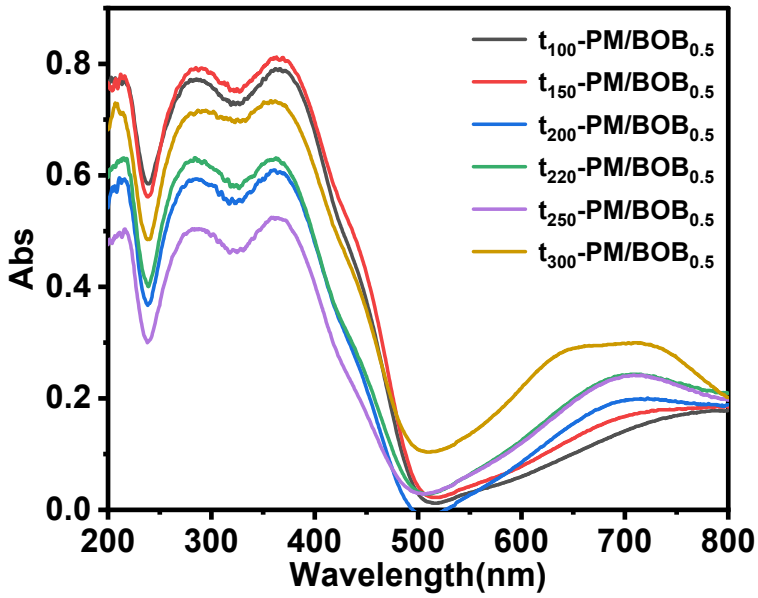

Fig. S5 UV-vis DRS spectra of t_n-PM/$BOB_{0.5}$ composites synthesized at different calcination temperatures

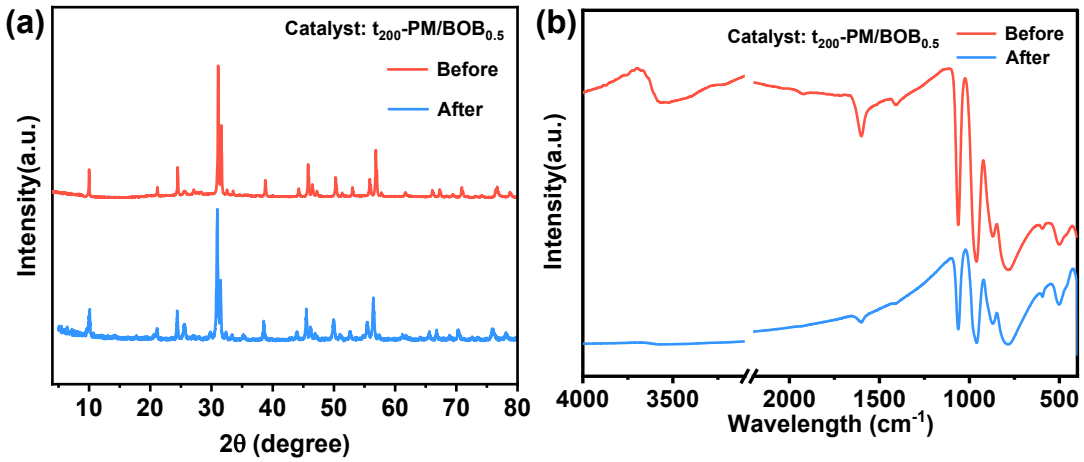

Fig.S6 Comparison of (a) XRD and (b) IR patterns of composite materials before and after photocatalytic CO_2 reduction reactions

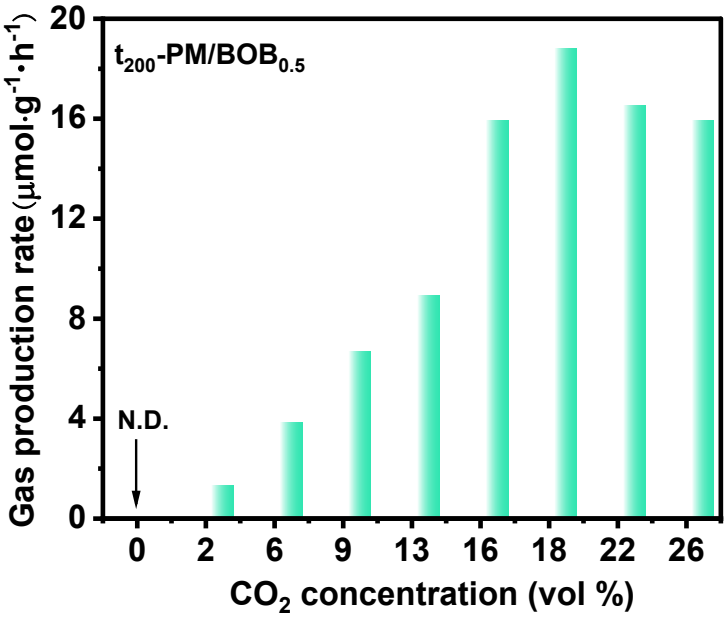

Fig. S7 The photocatalytic performance of t_{200}-PM/$BOB_{0.5}$ under varying CO_2 concentrations

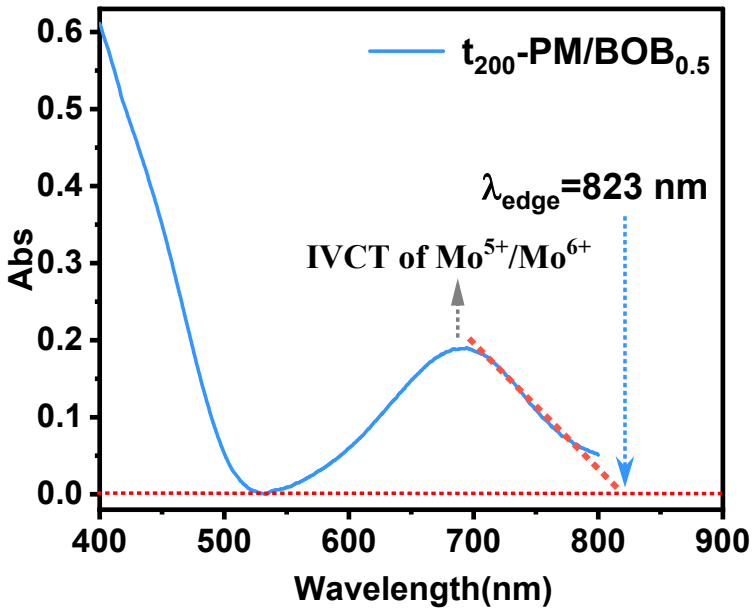

Fig. S8 The UV-vis DRS of t_{200}-PM/$BOB_{0.5}$

Table 1 Comparison of PCR performance with comparable materials under solid-gas mode

Light source	Photocatalyst	CO μmol·g^{-1}·h^{-1}	Refs.
A 300 W Xe lamp (AM 1.5)	**t_{200}-PM/$BOB_{0.5}$**	**18.82**	**This work**
A 300 W Xe lamp	8% P-BiOBr	9.13	Journal of Molecular Structure,

			2024, 1307: 138041
300 W Xe lamp	$BiOBr/NH_2$-UiO-66	9.2	Separation and Purification Technology, 2024, 344: 127289.
300 W Xe lamp (AM 1.5G filter)	$Bi_4O_5Cl_2$	14.6	ACS Catalysis, 2022, 12(7): 3965-3973.
300 W Xe lamp (420 nm cut-off filter)	BiOBr/CdS-5%	4.5	Separation and Purification Technology, 2022, 298: 121603.
300 W Xe lamp	NiTMCPP/BiOBr-2	2.8	Applied Catalysis B: Environment and Energy, 2025, 365: 124904.
300 W Xe lamp (λ > 420 nm)	$Ni_2P/NiO/CN$	1.51	J. Mater. Chem. A., 2022,10, 15752-15765
300 W Xe lamp	WO_{3-x}/In_2S_3-550	10	Angewandte Chemie International Edition, 2025, 64(2): e202414672.
300 W Xe lamp	$LaPO_4/g-C_3N_4$	14.43	Appl. Catal. B-Environ., 201 (2017) 629–635.
300 W Xe lamp	5 wt% $g-C_3N_4/CeO_2$	7.61	Journal of Rare Earths, 2024, 1002-0721
300 W Xe lamp (AM1.5)	Cu/CN-0.25	11.21	ACS Nano 2020., 14, 8584−8593
A 300 W Xe lamp	SiW_{12}-BiOBr	21	Sep. Purif. Technol. 2023, 321, 124228
A 300 W Xe lamp (full spectrum)	$\{CuI_8\}$ - $\{PMo_8V_6O_{42}\}$	20.06	Chem. Eng. J. 2022, 442, 136157
A 300 W Xe lamp (200 $mW{\cdot}cm^{-2}$)	SiW_{12}-Bi_2WO_6	16.2	Sep. Purif. Technol. 2023, 321, 124228
A 300 W Xe lamp (λ=300-1100nm, 200 $mW{\cdot}cm^{-2}$)	$\{M_3L_8\}$-$\{PMo_9V_7O_{44}\}$	15.5	JACS Au. 2021, 1, 8, 1288–1295
A 300 W Xe lamp (λ>400 nm)	Au@NENU-10	12.8	Adv. Mater. Interfaces, 2018, 5, 1801062.
200W Hg-Xe lamp with guidance fiber	Zn–Cr LDHs/SiW_{12}	0.05	Nanoscale Adv., 2024,6, 1241-1245